Inorganic Chemistry

Article

pubs.acs.org/IC

Kinetics Aspects of the Reversible Assembly of Copper in Heterometallic Mo_3CuS_4 Clusters with 4,4′-Di-*tert*-butyl-2,2′-bipyridine

Jose Ángel Pino-Chamorro,[†,⊥] Yuliya A. Laricheva,[‡,⊥] Eva Guillamón,[§,⊥] M. Jesús Fernández-Trujillo,[†] Andrés G. Algarra,[†] Artem L. Gushchin,[*,‡,§,∥] Pavel A. Abramov,[‡,§,∥] Emilio Bustelo,[*,†] Rosa Llusar,[*,§] Maxim N. Sokolov,[‡,∥] and Manuel G. Basallote[*,†]

[†]Departamento de Ciencia de los Materiales e Ingeniería Metalúrgica y Química Inorgánica, Facultad de Ciencias, and Instituto de Biomoléculas, INBIO, Universidad de Cádiz, Avda. República Saharahui s/n, Puerto Real, 11510 Cádiz, Spain

[‡]Nikolaev Institute of Inorganic Chemistry, Siberian Branch of the Russian Academy of Sciences, 630090 Novosibirsk, Russia

[§]Dept. de Química Física i Analítica, Universitat Jaume I, Av. Sos Baynat s/n, 12071 Castelló, Spain

[∥]Novosibirsk State University, 630090 Novosibirsk, Russia

Supporting Information

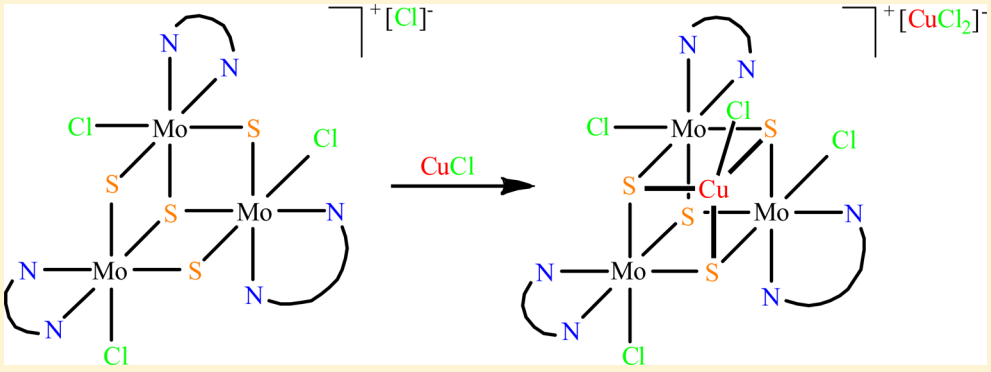

ABSTRACT: Treatment of the triangular $[Mo_3S_4Cl_3(dbbpy)_3]Cl$ cluster ([**1**]Cl) with CuCl produces a novel tetrametallic cuboidal cluster $[Mo_3(CuCl)S_4Cl_3(dbbpy)_3][CuCl_2]$ ([**2**][$CuCl_2$]), whose crystal structure was determined by X-ray diffraction (dbbpy = 4,4′-di-*tert*-butyl-2,2′-bipyridine). This species, which contains two distinct types of Cu(I), is the first example of a diimine-functionalized heterometallic $M_3M'S_4$ cluster. Kinetics studies on both the formation of the cubane from the parent trinuclear cluster and its dissociation after treatment with halides, supported by NMR, electrospray ionization mass spectrometry, cyclic voltammetry, and density functional theory calculations, are provided. On the one hand, the results indicate that addition of Cu(I) to $[\mathbf{1}]^+$ is so fast that its kinetics can be monitored only by cryo-stopped flow at −85 °C. On the other hand, the release of the CuCl unit in $[\mathbf{2}]^+$ is also a fast process, which is unexpectedly assisted by the $CuCl_2^-$ counteranion in a process triggered by halide (X^-) anions. The whole set of results provide a detailed picture of the assembly−disassembly processes in this kind of cluster. Interconversion between trinuclear M_3S_4 clusters and their heterometallic $M_3M'S_4$ derivatives can be a fast process occurring readily under the conditions employed during reactivity and catalytic studies, so their occurrence is a possibility that must be taken into account in future studies.

INTRODUCTION

A large variety of hetero-bimetallic cubane-type $M_3M'S_4$ (M = Mo, W) clusters with relevance in bio-inorganic chemistry and organic catalysis are known.[1−4] These species are easily accessible by direct incorporation of a metal atom in low oxidation state (zero to two) into homometallic M_3S_4 clusters (M = Mo, W). The success of the incorporation is greatly affected by the affinity of M′ for the bridging sulfur atoms and its reducing ability. With this strategy, a series of copper-incorporated cubane-type M_3CuS_4 complexes containing different types of ligands, such as aqua,[5−7] diphosphanes,[8,9] dithiophosphates,[8−10] dithiophosphinates,[11] cyclopentadienes,[12] dithiocarbamates,[13] acetates,[5] oxalates,[13] or acetylacetonates,[14] coordinated to the molybdenum or tungsten centers of the M_3CuS_4 unit have been synthesized with Cu(I) salts as Cu source. In addition, Mo(W)/Cu/S heterometallic clusters with different stoichiometries and a higher Cu content have been also prepared, some of them behaving as nonlinear optical materials.[15−19] Notably, the reactivity of some of these

Received: August 2, 2016
Published: September 22, 2016

DOI: 10.1021/acs.inorgchem.6b01878
Inorg. Chem. 2016, 55, 9912−9922

clusters has proven very interesting, as, for instance, the M_3CuS_4 clusters featuring diphosphane ligands have shown catalytic activity in the intra- and intermolecular cyclopropanation of diazo compounds.[8,9] A related M_3CuS_4 cluster containing hydride ligands has been shown to substitute the Cu-coordinated chloride by acetonitrile at a rate that increases in the presence of water as cosolvent, and the kinetico-mechanistic features of the process have been explored.[20] The high catalytic activity and selectivity of $[Mo_3S_4Cl_3(dmen)_3](BF_4)$ (dmen = *N*,*N*′-dimethylethylenediamine) in the reduction of nitroarenes to functionalized anilines has also been reported.[21] However, functionalization of M_3CuS_4 clusters (M = Mo, W) with diamine or diimine ligands such as 1,10-phenanthroline, 2,2′-bipyridine, and their derivatives was unexplored. Only recently, coordination of diimine ligands to the Mo_3S_4 cluster unit was reported.[22−24] In spite of their importance and the abundant literature on this kind of heterometallic clusters, the kinetico-mechanistic studies on the processes of interconversion between $M_3M'S_4$ clusters and their trimetallic precursors is limited to the reaction of $[M_3S_4(H_2O)_9]^{4+}$ (M = Mo, W) with Cu^+ in acidic water solutions.[7,25] Such information about the nature and reactivity of the products is of great interest, and it could be relevant for the design of homo- and heterogeneous catalysts. In fact, the M_3S_4 clusters can be considered as models for solid MoS_2 surfaces,[26] and thus the coordination/dissociation of a heterometal M′ is analogous to the adsorption of M′ metals on such surfaces. Vice versa, this process can also be viewed as the adsorption of a Mo_3S_4 cluster onto an M′ surface.[27]

Herein we report the synthesis and characterization of a new diimino cluster complex $[Mo_3(CuCl)S_4Cl_3(dbbpy)_3][CuCl_2]$, [**2**][$CuCl_2$], (dbbpy = 4,4′-di-*tert*-butyl-2,2′-bipyridine). To the best of our knowledge, [**2**][$CuCl_2$] represents the first example of a hetero-bimetallic $M_3M'S_4$ (M = Mo, W) cluster functionalized by a diimine ligand. The crystal structure of the cluster was determined by X-ray analysis and revealed the presence of a linear dichlorocuprate $[CuCl_2]^-$ anion as counterion. The paper also includes the results of kinetics studies on the interconversion between $[\mathbf{2}]^+$ and its $[Mo_3S_4Cl_3(dbbpy)_3]^+$ precursor that reveals an important role played by the counteranion. Nowadays, the influence of counterions in catalytic and stoichiometric reactivity is far from being considered "innocent", and even the ions considered "non-coordinating" can play unsuspected roles.[28−31] For example, ion pairing is significant in many organic solvents such as dichloromethane. In this context, counterions may have an impact upon both kinetics and selectivity of catalytic transformations, and occasionally, the effect of these can be advantageous.[32] Additionally, it is worth noting that synthetic procedures may, unintentionally, introduce metallic species that can be overlooked while having an impact on the outcome of the studied process, as shown in the case of the so-called "Silver Effect" in gold(I) catalysis.[33,34]

RESULTS AND DISCUSSION

Synthesis and Characterization. As commented above, hetero-bimetallic cuboidal $M_3M'S_4$ (M = Mo, W) clusters can be prepared by the reaction of incomplete cuboidal M_3S_4 clusters with other transition-metal complexes, where a metal atom (M′) is in low oxidation state. In the present case the high solubility of Mo_3S_4 complexes with 4,4′-di-*tert*-butyl-2,2′-bipyridine[24] allows to use this strategy for the synthesis of hetero-bimetallic Mo_3CuS_4 complexes. Thus, the reaction of the parent trinuclear complex $[Mo_3S_4Cl_3(dbbpy)_3]Cl$ ([**1**]Cl) with an excess of CuCl in tetrahydrofuran (THF) affords the desired $[Mo_3(CuCl)S_4Cl_3(dbbpy)_3][CuCl_2]$ ([**2**][$CuCl_2$]), product in ca. 80% yield. Crystals of solvate [**2**][$CuCl_2$]·$4CH_2Cl_2$ suitable for X-ray analysis were obtained by slow diffusion of hexane into dichloromethane solution. Figure 1 shows the molecular structure of the $[\mathbf{2}]^+$ cluster cation together with the $[CuCl_2]^-$ counterion. The metal core consists of a slightly distorted tetrahedral arrangement of one copper and three molybdenum atoms. Each tetrahedral face is capped by a μ_3-coordinated sulfide ligand generating a cuboidal structure. The coordination sphere around each Mo is essentially octahedral, consisting of two nitrogen atoms of a bipyridine ligand, three μ_3-S ligands, and a chloride. The tetrahedral environment around Cu in the cluster is defined by three μ_3-S ligands and a chloride.

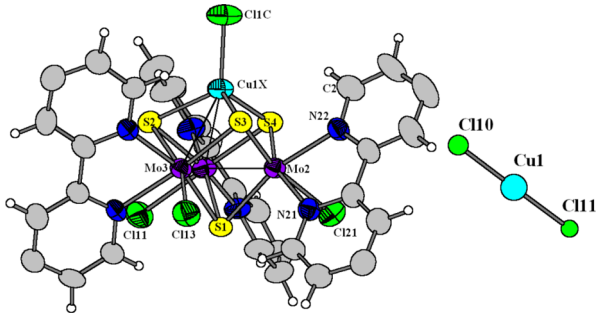

Figure 1. Ball-and-stick representation of the molecular structure of $[Mo_3(CuCl)S_4Cl_3(dbbpy)_3]^+$ ($[\mathbf{2}]^+$) cluster cation and $[CuCl_2]^-$ anion. Disordered *tert*-Bu groups are omitted for clarity. The average bond distances (Å): *d*(Mo−Mo) = 2.803(1), *d*(Mo−Cu) = 2.814(1), *d*(Mo−S_{Cu}) = 2.322(2), *d*(Mo−S_{Mo}) = 2.350(2), *d*(Cu−S) = 2.294(2), *d*(Cu−Cl) = 2.146(2), *d*(Mo−N) = 2.225(6); *d*(Cu−Cl) = 2.042(5) and 2.036(5) in $[CuCl_2]^-$.

Average Mo−Mo and Mo−Cu bond lengths of 2.803(1) and 2.814(1) Å, respectively, are similar to those found in other Mo_3CuS_4 clusters[12,35] and are consistent with the presence of M−M single bonds. Similarly to other chelating ligands, bipyridine is asymmetrically coordinated to the Mo_3S_4 core, with its nitrogen atoms cis and trans to the sulfur atom labeled as S1 in Figure 1 and bound to the three Mo centers. Interestingly, these trans and cis Mo−N bond lengths are approximately equal (the averaged value is 2.225(6) Å), whereas phenantroline coordination leads to Mo−N distances that differ by 0.1 Å in $[Mo_3S_4Cl_3(phen)_3]^+$.[22] Two distinctive sets of Mo−P bond distances have also been observed for the Mo_3CuS_4 diphosphine complexes.[36]

The Mo−N bond distances in $[Mo_3(CuCl)S_4Cl_3(dbbpy)_3]^+$ are very close to those found in $[Mo_3S_4Cl_3(dbbpy)_3]^+$ (2.237(8) Å),[24] $[Mo_3(\mu_3\text{-}S)(\mu_2\text{-}S_2)_3(dtc)_2(Me_2phen)]^{2+}$ (2.221(1), 2.210(1) Å),[37] and $[Mo_3(\mu_3\text{-}Se)(\mu_2\text{-}Se_2)_3(phen)_3]^{4+}$ (2.227(11), 2.237(11) Å)[38] but shorter than in $[Mo_3S_4Cl_3(phen)_3]^+$ (2.256(13) and 2.352(18) Å)[22] and $[Mo_3S_4(dtp)_2(\mu\text{-}AcO)Cl(Me_2bpy)]$ (2.2700(2) Å).[23] Moreover, despite the fact that no specific interactions between the $[Mo_3(CuCl)S_4Cl_3(dbbpy)_3]^+$ cation and the $[CuCl_2]^-$ anion are observed in the structure of [**2**][$CuCl_2$]·$4CH_2Cl_2$, the two Cu−Cl bond distances in the counterion are not identical, 2.042(5) and 2.036(5) Å, and slightly shorter than in other linear dichlorocuprates such as $[Cu(bipy)_2][CuCl_2]_2$ (2.091(2) Å, 180°), $[Cu(tmeda)_2][CuCl_2]$ (2.095(4), 180°), [Cu(1,10-

DOI: 10.1021/acs.inorgchem.6b01878
Inorg. Chem. 2016, 55, 9912−9922

phenanthroline)$_2$][CuCl$_2$] (2.0882(9), 2.0958(9), 178.75°),[39,40] and particularly that in the closely related cluster [Mo$_3$CuS$_4${(R,R)-Me-BPE}$_3$Cl$_4$][CuCl$_2$] ((+)-1,2-(R,R)-Me-BPE = bis[(2*R*,5*R*)-2,5-(dimethylphospholan-1-yl)]ethane): 2.067(13) and 2.103(12) Å, 180°. The Cu−Cl distance within the cation cluster is also shorter: 2.146(2) versus 2.180(10).[41]

The first M$_3$CuS$_4$ cluster unit reported, [Mo$_3$S$_4$(CuI)(dtp)$_3$(μ_2-CH$_3$CO$_2$)(DMF)] (dtp = diethyldithiophosphate), was prepared from [Mo$_3$S$_4$(dtp)$_4$(H$_2$O)] and CuI in DMF.[42] Since then, M$_3$CuS$_4$ clusters bearing many types of ligands referred to in the introduction section have been prepared. The complex reported in this work is the first example of a cuboidal cluster with the molybdenum atoms coordinated by diimine ligands. As it has been observed for other Mo$_3$CuS$_4$ clusters,[41] this compound is able to integrate a second Cu(I) unit as a [CuCl$_2$]$^-$ counterion (Scheme 1). Discrete monomeric dichlorocuprate anions frequently occur in nonaqueous solvents but can be isolated in the solid state only in combination with relatively large cations.[39]

Scheme 1. Simplified Scheme[a] for the Synthesis of [2][CuCl$_2$]

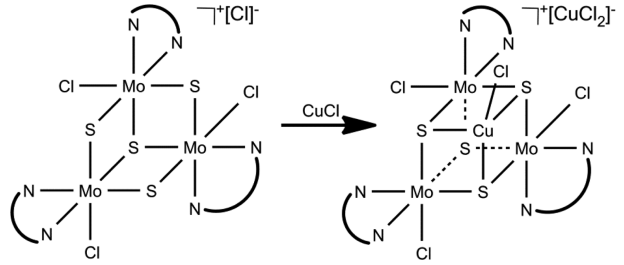

[a]M−M bonds are omitted for clarity.

Compound [2][CuCl$_2$] has also been characterized by electrospray ionization mass spectrometry (ESI-MS) and by ^{1}H and ^{13}C{^{1}H} NMR techniques. The ESI mass spectrum, recorded at U_c = 20 V in a CH$_2$Cl$_2$/CH$_3$CN mixture (Figure 2a), reveals the pseudomolecular peak of [2]$^+$ cation at m/z = 1427 together with a peak at m/z = 1328 resulting from the loss of CuCl in the cluster.[43] As the NMR spectrum of compound [2][CuCl$_2$] (see Experimental Section) gives no evidence of the dissociation of CuCl in solution, we assume that the release of CuCl takes place under ESI-MS conditions. This behavior is in fact not unprecedented, and it has been observed, although at higher cone voltages (U_c = 70−90 V), for [M$_3$CuS$_4$X$_3$(diphosphine)$_3$]$^+$ (M = Mo, W; X = Cl, Br, H) complexes.[20,36] Notably, in these diphosphino analogues the loss of the CuCl moiety occurs simultaneously with that of a neutral diphosphine.

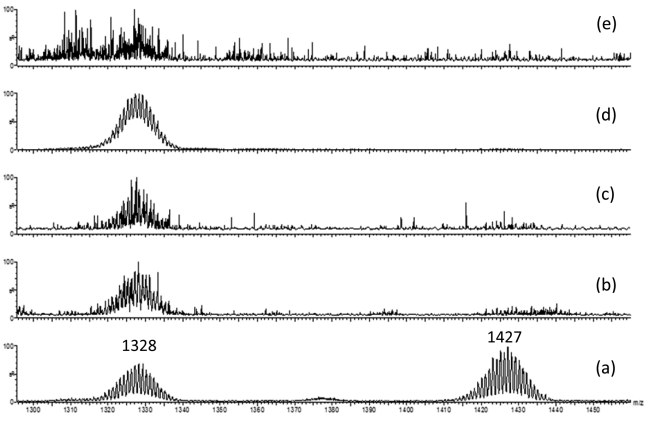

Figure 2. Mass spectra (positive scan) at U_c = 20 V in CH$_2$Cl$_2$/CH$_3$CN for [2][CuCl$_2$] (a) and for the products of the reactions with Cl$^-$ (b), Br$^-$ (c), stoichiometric F$^-$(d), and excess of F$^-$ (e).

The cyclic voltammogram of [2][CuCl$_2$] in CH$_3$CN (Figure 3) shows a quasi-reversible one-electron reduction process at

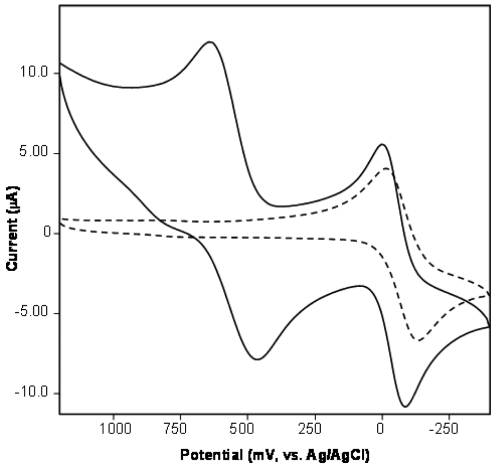

Figure 3. Cyclic voltammograms of 1 mM solution of [2][CuCl$_2$] (solid line) and 1 mM solution of [2](PF$_6$) (dashed line) in the presence of 0.05 M solution of Bu$_4$NPF$_6$ between 1.2 ↔ −0.4 at 0.1 V·s^{-1} scan rate.

$E_{1/2}$ = −0.047 V (vs Ag/AgCl) within the sweeping range between 0 and −2 V. The ΔE_p value was calculated as 0.077 at 0.1 V s^{-1} scan rate, and it increases with an increase in the scan rate, thus indicating a quasi-reversibility of the process. The corresponding reversible one-electron reduction process for the trinuclear precursor [Mo$_3$S$_4$Cl$_3$(dbbpy)$_3$]Cl is found at $E_{1/2}$ = −0.408 V (ΔE_p = 0.077 V, vs Ag/AgCl; see Figure S1). This corresponds to an anodic shift of the redox potential by ca. 0.36 V upon copper incorporation and is consistent with the M$_3$CuS$_4$ clusters being reduced more easily than the parent M$_3$S$_4$ cluster. According to the generally accepted interpretation,[44] the one-electron reduction of [Mo$_3$(CuCl)S$_4$Cl$_3$(dbbpy)$_3$]$^+$ is regarded as the Mo$^{IV}_3$Cu^I↔Mo^{III}Mo$^{IV}_2$Cu^I process centered on molybdenum. However, we have recently shown that the reduction of Mo$_3$S$_4$ clusters coordinated to noninnocent phenanthroline or bipyridine ligands causes electron density delocalization over the ligand and the Mo center,[22] and therefore the reduction of [Mo$_3$(CuCl)S$_4$Cl$_3$(dbbpy)$_3$]$^+$ can also be considered as both metal- and ligand-centered. Density functional theory (DFT) calculations[45] for [Mo$_3$(CuCl)S$_4$Cl$_3$(bpy)$_3$]$^+$ ([**1t**]$^+$) and the reduced species [Mo$_3$(CuCl)S$_4$Cl$_3$(bpy)$_3$] ([**1t**]) support this attribution, as the highest occupied molecular orbital (HOMO) of the latter is significantly more localized at one of the three Mo(bpy) units of the cluster, although still predominantly at the Mo center (see Figure S2 and Tables S1 and S2 in the Supporting Information). In contrast, the contributions from the sulfur atoms and the heterometallic CuCl unit remain practically unaffected. It is worth noting that the reduction potential of [Mo$_3$(CuCl)S$_4$Cl$_3$(dbbpy)$_3$]$^+$ ($E_{1/2}$ = −0.047 V) is much higher than the first reduction potential of [Mo$_3$(CuCl)S$_4$Cl$_3$(dmpe)$_3$]$^+$ ($E_{1/2}$ = −0.31 V) and [Mo$_3$(CuI)S$_4$Cp*$_3$]$^+$

DOI: 10.1021/acs.inorgchem.6b01878
Inorg. Chem. 2016, 55, 9912−9922

($E_{1/2}$ = −0.82 V), which shows that the redox properties of these clusters are greatly affected by the ligands attached to Mo. An oxidation process is also observed at $E_{1/2}$ = 0.55 V (ΔE_p = 0.55 V, vs Ag/AgCl). This can be attributed to the one-electron oxidation of Cu(I) to Cu(II) in $[CuCl_2]^-$ counterion, as the redox potential is very close to that observed for the $[Cu^{II/I}(CH_3CN)_4]^{2+/+}$ couple (0.57 V, vs Ag/AgCl).[46]

It is worth noting that the reaction of the PF_6^- salt of the trimetallic precursor, [**1**](PF_6), with CuCl yields a mixture of compounds. However, an alternative synthetic approach to a salt of $[\mathbf{2}]^+$ without the $[CuCl_2]^-$ anion was successfully performed by passing a solution of [**2**][$CuCl_2$] through a silica gel column with a saturated solution of KPF_6 in acetone as eluent. The resulting [**2**](PF_6) exhibits ^{1}H NMR signals identical with [**2**][$CuCl_2$]. The presence of the PF_6^- is evident from its characteristic doublet in ^{19}F NMR signals and characteristic frequency values in the IR spectrum. Consequently with the interpretation above, the cyclic voltammogram of [**2**](PF_6) only shows a reduction process at $E_{1/2}$ = −0.071 V (ΔE_p = 0.107 V, vs Ag/AgCl) in CH_2Cl_2 (Figure 3).

The Reaction of the Heterometallic $[\mathbf{2}]^+$ Cluster with Halides in Dichloromethane. As a logical follow-up to our previous studies on halide substitution kinetics on Mo and W clusters,[47−49] the reactivity of the cluster [**2**][$CuCl_2$] was tested against an excess of tetraalkylammonium or phosphonium halide and pseudohalide (thiocyanate) salts. Initial experiments in CH_3CN indicated that the cluster is not stable in this solvent under the conditions of the stopped-flow experiments, and so kinetics studies were performed in CH_2Cl_2. Surprisingly, preliminary kinetics experiments in the latter solvent showed that [**2**][$CuCl_2$] reacts with Cl^- with spectral changes similar to those observed for the reaction with other anions. The electronic absorption spectrum of the starting compound [**2**][$CuCl_2$] features a band centered at 509 nm (Figure S3), and addition of an excess of Pr_4NCl, Bu_4PBr, or Bu_4NF in dichloromethane causes the disappearance of this characteristic band (Figure 4). The reaction with fluoride features additional

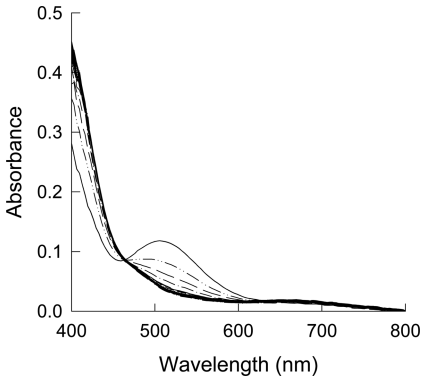

Figure 4. Typical spectral changes for the reaction of [**2**][$CuCl_2$] with Pr_4NCl in CH_2Cl_2 at 25.0 °C ([cluster] = 3.5 × 10^{-5} M, [Pr_4NCl] = 3.7 × 10^{-4} M, experiment time = 0.4 s).

slower spectral changes with a complex behavior that reveals the occurrence of additional kinetics steps corresponding to subsequent reactions whose kinetics was too complex to be analyzed. Nevertheless, in all cases fast spectral changes are observed within the time scale of the stopped-flow technique, and these can be satisfactorily fitted to a model with a single kinetic step. The calculated spectra for the starting complex and the reaction product with Pr_4NCl are shown in Figure S4, and comparison of the latter with the spectrum of a pure sample of $[\mathbf{1}]^+$ suggests that the observed process consists of CuCl dissociation. Reaction with thiocyanate exhibits a similar behavior, but the process is so fast that it ends within the stopped-flow mixing time, thus precluding the acquisition of kinetics data.

As the final spectra suggest the formation of the trinuclear cluster $[\mathbf{1}]^+$ as the reaction product, additional experimental evidence was obtained via NMR and ESI-MS techniques. Thus, addition of Pr_4NCl, Bu_4PBr, or $Bu_4N(SCN)$ in excess (0.09 M in the NMR tube) to a diluted solution of [**2**][$CuCl_2$] (3.5 × 10^{-3} M) in CD_2Cl_2 causes an immediate color change from red to yellow. The process yields the parent trinuclear cluster $[\mathbf{1}]^+$, as inferred by comparison of the ^{1}H NMR bipyridine chemical shifts of the resulting compound with those of a fresh sample of $[\mathbf{1}]^+$.[24] In all cases six nonequivalent multiplets appear, corresponding to three symmetric {Mo(dbbpy)} moieties featuring asymmetrically coordinated bipyridine ligands (see Figure S5a,b). ESI mass spectrometric analysis in positive and negative modes was used to determine the molecular mass of the species appearing under experimental conditions similar to those in the kinetics and NMR measurements. Figure 2b−e shows the ESI-MS (positive mode) spectra of the products obtained upon reaction between [**2**][$CuCl_2$] and the different halide salts. Addition of chloride, bromide, or fluoride salts produces dissociation of the CuCl moiety to afford the trinuclear $[\mathbf{1}]^+$ cation, evidenced by the peak at m/z = 1328. Negative scans show a mixture of chlorocuprate species $[CuCl_2]^-$, $[Cu_2Cl_2]^-$, and $[CuCl_3]^-$. Upon chloride addition as Pr_4NCl salt, the intensities of these signals increase (see Supporting Information, Figure S6b). Similarly, when a bromide salt is added, mixed halocuprates species $[CuClBr]^-$, $[CuCl_2Br]^-$, and $[CuClBr_2]^-$ are registered together with the $[CuBr_2]^-$ anion and minor amounts of $CuCl_2^-$ and $CuCl_3^-$. Upon addition of Bu_4NF salt, $[CuCl_2]^-$ is the major anion detected. Treatment of [**2**](PF_6) with Bu_4PBr yields the $[CuBr_2]^-$, $[CuClBr]^-$, $[CuCl_2Br]^-$, and $[CuClBr_2]^-$ species (see Figure S7). A mixture of [**2**](PF_6) and thiocyanate (as $Bu_4N(NCS)$) exhibits the peak from $[\mathbf{1}]^+$ in positive scans and $[Cu(SCN)_2]^-$ and $[CuCl(SCN)]^-$ in the negative side.

The kinetics study of the reactions between [**2**][$CuCl_2$] and an excess of Pr_4NCl, Bu_4PBr, or Bu_4NF shows that the processes take place in a single kinetic step, with the values of the observed rate constants k_{obs} exhibiting a linear dependence on the halide concentration (Figure 5). Fitting of these to eq 1

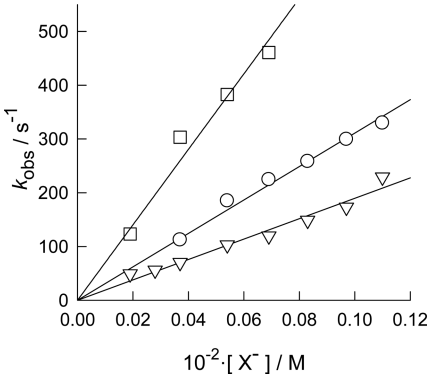

Figure 5. Halide concentration [X^-] vs k_{obs} plots for the reaction of [**2**][$CuCl_2$] with Bu_4NF (□), Pr_4NCl (▽), and Bu_4NBr (○) in CH_2Cl_2. Solid lines correspond to the data fitting by eq 1.

DOI: 10.1021/acs.inorgchem.6b01878
Inorg. Chem. 2016, 55, 9912−9922

leads to second-order rate constants of $k_1 = (190 \pm 6) \times 10^3$ M^{-1} s^{-1} for chloride, $(311 \pm 5) \times 10^3$ M^{-1} s^{-1} for bromide, and $(702 \pm 29) \times 10^3$ M^{-1} s^{-1} for fluoride. The rate constant for reaction with thiocyanate must be higher, as deduced from the occurrence of reaction within the stopped-flow mixing time. Notably, although the process is comparatively slower with chloride and bromide than with fluoride ($F^- > Br^- > Cl^-$), the differences are not very large. The ordering of the different entering ligands is probably a consequence of a complex balance between different factors that include outer sphere complexation of the cluster with one or more anions, secondary reactions of the entering anion with the $[CuCl_2]^-$ counterion, and possible changes in the substitution mechanism, as will be commented below for the case of fluoride.

$$k_{1obs} = k_1[X^-] \quad (1)$$

It is remarkable that no halide exchange occurs at the Mo centers regardless of the entering halide, except for fluoride or the counterion in these trinuclear and tetranuclear cuboidal clusters. These experiments confirm the loss of CuCl from the initial hetero-bimetallic cluster upon treatment with chloride, bromide, and thiocyanate salts without altering the rest of the trinuclear cluster structure. These findings are surprising in view of our previous results for the related $[W_3(CuCl)S_4H_3(dmpe)_3]^+$,[49] which undergoes substitution of the Cu-coordinated chloride without disassembly of the heterometallic cluster. To gain further insight into this question we employed DFT methods to compute the reaction free energies associated with the elimination of $[CuCl_2]^-$ at $[W_3(CuCl)S_4H_3(dmpe)_3]Cl$, $[W_3(CuCl)S_4Cl_3(dmpe)_3]Cl$, and $[Mo_3(CuCl)S_4Cl_3(bpy)_3]Cl$, the latter employed as a model for [**2**]Cl. The results, included in Table 1, indicate that $[CuCl_2]^-$ elimination is an endergonic process in all cases, so that experimentally it is probably driven both by the excess of halide and the subsequent transformations that the resulting $[CuCl_2]^-$ can undergo. In any case, it is notable that the process is thermodynamically more favorable for $[Mo_3(CuCl)S_4Cl_3(bpy)_3]Cl$ than for $[W_3(CuCl)S_4H_3(dmpe)_3]Cl$, in agreement with the experimentally confirmed lack of $[CuCl_2]^-$ elimination at the latter species. Interestingly, substitution of hydride by chloride ligands at $[W_3(CuCl)S_4H_3(dmpe)_3]Cl$ to yield $[W_3(CuCl)S_4Cl_3(dmpe)_3]Cl$ leads to a decrease on the stability of the cluster toward $[CuCl_2]^-$ elimination up to a ΔG_r similar to that of $[Mo_3(CuCl)S_4Cl_3(bpy)_3]Cl$. Unfortunately, although this could be indicative of $[CuCl_2]^-$ elimination at $[W_3(CuCl)S_4Cl_3(dmpe)_3]Cl$, its reactivity has never been studied in detail, and therefore definite conclusions cannot be drawn.

Table 1. Summary of Reaction Gibbs Free Energies Calculated in Acetonitrile Solution for the Elimination of $[CuCl_2]^-$ at $[W_3(CuCl)S_4H_3(dmpe)_3]Cl$, $[W_3(CuCl)S_4Cl_3(dmpe)_3]Cl$, and $[Mo_3(CuCl)S_4Cl_3(bpy)_3]Cl$

reaction	ΔG_r[a]
$[W_3(CuCl)S_4H_3(dmpe)_3]^+\cdots Cl^- \rightarrow [W_3S_4H_3(dmpe)_3]^+\cdots CuCl_2^-$	25.1
$[W_3(CuCl)S_4Cl_3(dmpe)_3]^+\cdots Cl^- \rightarrow [W_3S_4Cl_3(dmpe)_3]^+\cdots CuCl_2^-$	19.9
$[Mo_3(CuCl)S_4Cl_3(bpy)_3]^+\cdots Cl^- \rightarrow [Mo_3S_4Cl_3(bpy)_3]^+\cdots CuCl_2^-$	19.2

[a]In kilocalories per mole.

However, NMR experiments indicate that the reaction of [**2**][$CuCl_2$] with Bu_4NF leads to a more symmetrical chemical environment for the dbbpy ligands, as only three signals appear in the aromatic region (see Supporting Information, Figure S5c). Surprisingly, the parent trinuclear cluster [**1**]Cl also reacts with fluoride generating a compound that shows the same ^1H NMR. The chemical shifts of these signals match well with those of free dbbpy, thus suggesting that the dbbpy ligands are released upon treatment with fluoride excess. The $^{13}C\{^1H\}$ NMR spectrum shows signals at δ 118.3, 121.1, 149.2, 156.6, and 161.2 ppm, which also match well with the expected resonances for the free ligand. It has been reported that related trinuclear clusters $[M_3S_4F_3(dppe)_3]^+$ (M = Mo, W; dppe = 1,2-bis(diphenylphosphinoethane)) can be prepared from $[Mo_3S_4Cl_3(dppe)_3](PF_6)$ through halogen substitution reactions by using an excess of CsF and heating at 60 °C during 24 h.[50] These observations confirm the higher reactivity of fluoride with the analogous diphosphine M_3S_4 derivatives, although in that case diphosphine release is not observed in the presence of fluoride excess.

ESI-MS experiments (Figure 2e) indicate that reaction with an excess of F^- leads to the disappearance of the signals for both $[\mathbf{2}]^+$ and $[\mathbf{1}]^+$, in agreement with extensive cluster transformations involving dbbpy release. It is interesting to note that after addition of a limited amount of F^- (Figure 2d), ESI-MS still shows clearly the signal of $[\mathbf{1}]^+$, thus suggesting that the whole process starts similarly for all halides (thus $[\mathbf{2}]^+ \rightarrow [\mathbf{1}]^+$ as the first step). This explains the similar kinetics data observed for fluoride with respect to chloride and bromide. According to this hypothesis the slow spectral changes observed after the initial kinetic step and the ESI-MS changes produced on adding an excess of fluoride can be explained by the consecutive reaction of the trinuclear $[\mathbf{1}]^+$ cluster with fluoride. This conclusion is confirmed by reacting [**1**]Cl with the halide salts. Thus, whereas $[\mathbf{1}]^+$ remains stable upon treatment with chloride and bromide, the cluster peak (m/z = 1328) disappears after treatment with Bu_4NF. Negative scans of mass spectra show the $[CuCl_2]^-$ species as the major component. These results confirm that the subsequent spectral changes observed in the kinetics experiments with fluoride are caused by reactions of the trinuclear cluster $[\mathbf{1}]^+$.

Stopped-flow experiments (Figures S8 and S9) confirmed that the reaction of $[\mathbf{1}]^+$ with fluoride excess is a complex polyphasic process that involves extensive transformations of the cluster core, but a detailed kinetics study was not performed because of the exceedingly complex spectral changes. Instead, DFT calculations were used to analyze the mechanism of substitution of chloride by fluoride and bromide ligands at $[Mo_3S_4Cl_3(bpy)_3]^+$ ($[\mathbf{1t}]^+$). The results, included in the Supporting Information, indicate that the nature of the entering ligand has a strong impact on the characteristics of these substitution processes, with associative and dissociative mechanisms being favored for fluoride and bromide, respectively. From an energetic viewpoint, the substitution is computed to be both kinetically and thermodynamically more favored when fluoride is the entering ligand, which agrees with the experimental results.

In summary, the addition of chloride, bromide, or thiocyanate salts to [**2**][$CuCl_2$] induces the release of the copper chloride unit, maintaining the Mo_3S_4 core, whereas the addition of fluoride leads to further transformations that include the release of the bipyridine ligand and probably the Mo-coordinated chloride ligands. In such case the ultimate product could be $[Mo_3S_4F_9]^{5-}$.[51] Nevertheless the experimental

DOI: 10.1021/acs.inorgchem.6b01878
Inorg. Chem. 2016, 55, 9912−9922

Scheme 2. Alternative Mechanistic Pathways for the Counteranion-Induced Release of Copper Chloride at [2][CuCl$_2$]

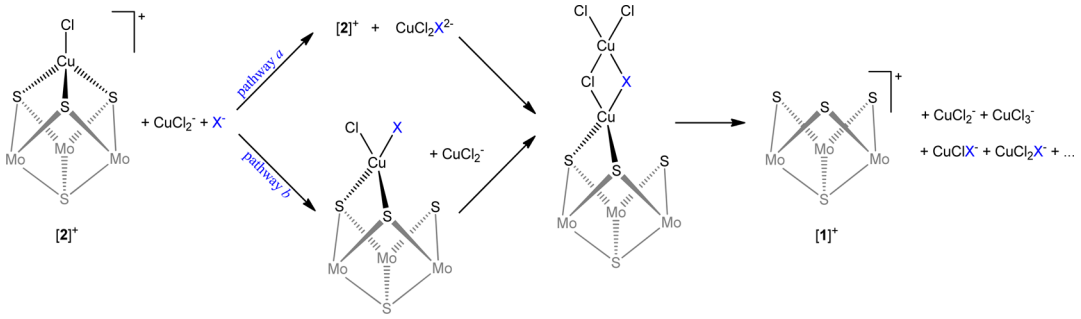

data indicate that the reaction of [**2**]$^+$ with fluoride starts in the same way that the reaction starts with other halides.

To check the possible effect of [CuCl$_2$]$^-$ counterions on the process, some experiments were performed using [**2**](PF$_6$). Thus, although the ^{1}H NMR spectra of [**2**][CuCl$_2$] and [**2**](PF$_6$) are essentially equal, their UV−vis spectra are different (Figure S3), and therefore this must be related to the presence of the [CuCl$_2$]$^-$ counterion. Moreover, NMR monitoring of the reactions with chloride and bromide salts unexpectedly showed that their reactions with [**2**](PF$_6$), if occurring at all, are substantially slower than those observed with [CuCl$_2$]$^-$ as counterion. Accordingly, stopped-flow experiments on the reaction with chloride and bromide sources using [**2**](PF$_6$) show much slower spectral changes than those of [**2**][CuCl$_2$]. Moreover, these are so small that a satisfactory kinetics analysis is not possible. Nevertheless, formation of the trinuclear cluster [**1**]$^+$ is observed in the reaction of [**2**](PF$_6$) with thiocyanate, thus showing that copper release does not require the assistance of [CuCl$_2$]$^-$ in order to take place. In any case, these experiments show an unprecedented and important effect of the counterion on the kinetics of disassembly of the heterometallic cluster.

The kinetics study is tied to a common spectroscopic feature, namely, the disappearance of the UV−vis band at 509 nm, characteristic of [**2**]$^+$. This spectral change is related to the copper release from the cluster, and although in the case of thiocyanate it occurs without the assistance of the [CuCl$_2$]$^-$ counteranion, this counterion plays an active role in the heterometallic cluster breakage, a process that is induced by halide excess. A question that arises at this point is the nature of the rate-determining step (r.d.s.) in this process. Substitution of the Cu-coordinated chloride ligand in [**2**]$^+$ by X$^-$ appears unlikely because cluster demetalation with chloride occurs at a rate similar to other anions, and thence alternative mechanisms must be invoked. One possibility is that the r.d.s. corresponds to the attack of X$^-$ at the CuCl$_2^-$ anion to form CuCl$_2$X^{2-} (pathway *a* in Scheme 2), which could then attack the CuCl unit in [**2**]$^+$. Adding to this point, it has been shown that in aqueous chloride media, copper(I) species [CuCl$_2$]$^-$ and [CuCl$_3$]$^{2-}$ are in equilibrium. This has been evidenced by the increase in peak absorption at 274 nm with increased chloride concentration,[52] but unfortunately, in the present case this region is obscured by the UV band from [**2**][CuCl$_2$]. It seems plausible nonetheless to consider this equilibrium to be responsible for the CuCl abstraction from the cluster to yield a [Cu$_2$Cl$_3$]$^-$ anion, which is often found in compounds with relatively small cations such as (Me$_4$N)[Cu$_2$Cl$_3$].[33] Once the binuclear anion is released, a complex speciation is expected to occur in solution with formation of a variety of copper halide species depending on the conditions,[53] with Cu(I)−Cu(II) oxidation processes further shifting the equilibrium toward [**2**]$^+$ decomposition, as observed by ESI-MS.

An alternative possibility that shares common features with the previous one is an associative attack of X$^-$ to the Cu−Cl unit in the cluster (pathway *b* in Scheme 2). This type of process has been observed for the chloride substitution at [W$_3$CuClS$_4$H$_3$(dmpe)$_3$]$^+$ and it has been shown to occur with a cluster reorganization that involves the cleavage of a Cu−S bond to accommodate for the excess of electron density introduced by the additional ligand.[20] Subsequent X$^-$ attacks could then lead to Cu removal in a process that does not require the assistance of the [CuCl$_2$]$^-$ counterion. However, pathway *b* only appears to be efficient enough to be observed in the case of thiocyanate, as this is the only anion for which the reaction has been observed with [**2**](PF$_6$). In the presence of other anions, the operation of the [CuCl$_2$]$^-$ assisted pathway *a* is more effective. In that case, [CuCl$_2$]$^-$ attack to the CuClX unit in the cluster would lead to a dinuclear species of the type previously invoked. All in all, regardless of the precise details, it appears that it is the capability of Cu(I) to form dinuclear species with bridging anions[54−56] what facilitates the counteranion assisted pathway.

The Formation of the Heterobimetallic Cuboidal Cluster. Once the kinetic and mechanistic features associated with the release of CuCl from [**2**]$^+$ and the important role of the counteranion were established, efforts were made to obtain kinetics information about the reverse process, that is, copper addition to the trinuclear cluster to form [**2**]$^+$. Although the synthesis of [**2**][CuCl$_2$] was performed by reaction of [**1**]Cl with CuCl in THF or CH$_3$CN, the insolubility of the copper reagent in most solvents makes it unfeasible to study the reaction kinetics in solution. For this reason, stopped-flow studies on the formation of the heterometallic [**2**]$^+$ cluster were initially performed by monitoring the reaction of the trimetallic [**1**]Cl cluster with [Cu(CH$_3$CN)$_4$]BF$_4$ in dichloromethane. The addition of [Cu(CH$_3$CN)$_4$]BF$_4$ to solutions of [**1**]Cl leads to an instantaneous color change from green to dark orange. However, experiments performed at 25 °C show that already the first spectrum recorded immediately after mixing in the stopped-flow instrument (ca. 1.7 ms of reaction time) does not correspond to the starting trinuclear cluster but to the reaction product. Similar experiments were therefore performed using a cryo-stopped flow system at low temperature in acetone. Surprisingly, even at −85 °C the reaction was found to be extremely rapid under pseudo-first-order conditions and again the initial recorded spectrum did not correspond to the starting cluster. In fact, suitable spectral changes were only obtained following the reaction at −85 °C with a small excess of

DOI: 10.1021/acs.inorgchem.6b01878
Inorg. Chem. 2016, 55, 9912−9922

$[Cu(CH_3CN)_4]^+$ (Figure 7). These showed the appearance of a band centered at 480 nm, and the spectral changes could be

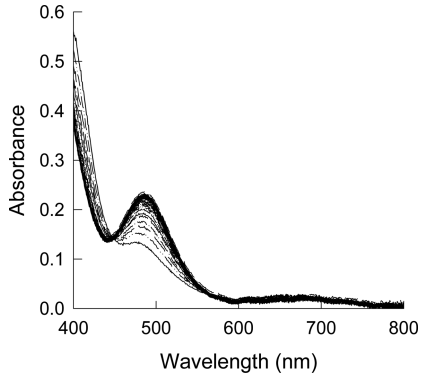

Figure 7. Typical spectral changes for the reaction of [**1**]Cl with $[Cu(CH_3CN)_4]BF_4$ in acetone at −85.0 °C ([**1**] = 1.4×10^{-4} M, $[[Cu(CH_3CN)_4]BF_4] = 7 \times 10^{-4}$ M, experiment time = 0.75 s).

satisfactorily fitted to a single kinetic step model with a second-order rate constant of $k = (2.63 \pm 0.05) \times 10^4$ M^{-1} s^{-1} at −85 °C. It is noteworthy that very small and much slower spectral changes are observed when the reaction is performed in the presence of an excess of Pr_4NCl, which suggests that the chloride excess inhibits the formation of the hetero-bimetallic cluster, in agreement with the results in the previous section. The value derived in the present work for the addition of Cu(I) to the trinuclear cluster is significantly faster (ca. 1×10^4 M^{-1} s^{-1} at −85.0 °C) than those previously reported for the reaction of $[M_3S_4(H_2O)_9]^{4+}$ clusters (M = Mo, W) with Cu^+ in acidic water solution (ca. 1×10^3 M^{-1} s^{-1} at 25.0 °C).[7,25] Although the difference could be due to the very different nature of the clusters and solvent, the possibility of some interference in the previous study caused by the instability of Cu^+ in water cannot be ruled out.

The formation of the heterometallic cubane-type cluster under conditions similar to those used in the kinetics experiments was confirmed by NMR and ESI-MS experiments. Thus, on the one hand, ^1H NMR experiments show the appearance of the pattern for the dbbpy aromatic hydrogen atoms characteristic of $[\mathbf{2}]^+$ (Figure S5a). On the other hand, positive scan ESI-MS spectra of reaction of $[\mathbf{2}]^+$ with an excess of $[Cu(CH_3CN)_4]BF_4$ complex (Figure 8 middle) indicate the formation of mixed chloride/fluoride tetranuclear species $[Mo_3(CuCl)S_4Cl_2\mathbf{F}(dbbpy)_3]^+$, $[Mo_3(CuCl)S_4Cl\mathbf{F}_2(dbbpy)_3]^+$, and $[Mo_3(CuCl)S_4\mathbf{F}_3(dbbpy)_3]^+$ at m/z = 1410, 1394, and 1377, respectively. Peak assignments were based on the m/z values and their characteristic isotopic pattern (Figure S10). Thus, it seems that in the absence of an external chloride source the softer Cu center abstracts a chlorine atom from one of the Mo−Cl bonds, which is replaced by Mo−F, in accordance with the harder character of Mo in the cluster. This conclusion is confirmed by recording the mass spectrum in the presence of a stoichiometric amount of Cl^- (Figure 8 top), which only shows the pseudomolecular peak attributed to the $[Mo_3(CuCl)S_4Cl_3(dbbpy)_3]^+$ cation.

CONCLUSION

The novel heterometallic cluster $[\mathbf{2}][CuCl_2]$ has been synthesized by the reaction of [**1**]Cl with an excess of CuCl, and reactivity studies have led to unforeseen and interesting results due to the presence of two chemically distinct Cu(I) centers. The studies performed represent, to the best of our knowledge, the first comprehensive kinetics study on the formation of heterometallic clusters and their ulterior demetalation processes as a result of the addition of halide and pseudohalide salts. Unlike other related compounds, $[\mathbf{2}][CuCl_2]$ regenerates the parent trinuclear cluster $[Mo_3S_4Cl_3(dbbpy)_3]^+$ upon treatment with halide and pseudohalide salts in a process that is assisted by the presence of the Cu(I) counterion. As both the trinuclear Mo cluster and the released Cu(I) species are capable of catalytic transformations of organic molecules, the reported process could be viewed as a new method to generate in situ stoichiometric amounts of them. On the one hand, the process is somewhat more complicated in the case of fluoride because of subsequent reactions of this anion with $[Mo_3S_4Cl_3(dbbpy)_3]^+$. On the other hand, addition of Cu(I) to this cluster is so fast that it could only be monitored by working at relatively low temperature. As a whole, the results indicate that the interconversion between M_3S_4 and $M_3M'S_4$ clusters can be very fast, thus providing unexpected reaction pathways for both of them. The presence of M_3S_4 clusters when dealing with their heterometallic $M_3M'S_4$ derivatives, and vice versa, should therefore be carefully checked in future reactivity and catalytic studies.

EXPERIMENTAL SECTION

General Procedures. All reactions were performed under inert atmosphere, unless otherwise stated. Starting complexes $[Mo_3S_4Cl_3(dbbpy)_3]Cl$ ([**1**]Cl) and $[Mo_3S_4Cl_3(dbbpy)_3](PF_6)$ ([**1**]-

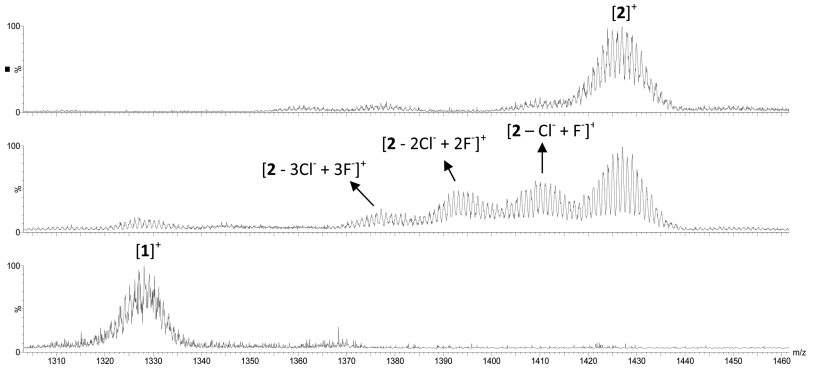

Figure 8. ESI-MS (positive scan) at U_c = 20 V for pure [**1**]PF_6 (bottom), a mixture of [**1**]PF_6 with $[Cu(MeCN)_4]BF_4$ (middle), and [**1**]PF_6 with $[Cu(MeCN)_4]BF_4$ and Pr_4NCl (top).

DOI: 10.1021/acs.inorgchem.6b01878
Inorg. Chem. 2016, 55, 9912−9922

(PF_6)) were prepared according to the published procedures.[24] All other reagents were obtained from commercial sources and used as received. Organic solvents were dried by standard methods before use.

Physical Measurements. Elemental analyses were performed with a EuroEA3000 Eurovector analyzer. The ^1H and ^{13}C NMR spectra were recorded with a Bruker Avance 500 spectrometer at room temperature. The shifts of the residual protons of the deuterated solvent (CD_2Cl_2 or $CDCl_3$) were used as an internal reference. A triple quadrupole mass spectrometer with an orthogonal Z-spray source (Waters, Manchester) was used. The temperature of the source block was set to 100 °C, and the desolvation temperature was set to 120 °C. A capillary voltage of 3.3 kV was used in the positive scan mode or 1.1 kV in the negative scan mode, and the cone voltage was set to U_c = 20 V. Mass calibration from m/z = 50 to 3000 was performed with a solution of sodium iodide in 2-propanol/water (50:50). Sample solutions in CH_2Cl_2/CH_3CN or CH_2Cl_2 were injected with a syringe pump directly connected to the ESI source at a flow rate of 10 μL min^{-1}. The observed isotopic pattern of each compound perfectly matched the theoretical isotope pattern calculated from their elemental composition by using the MassLynx 4.1 program. The cyclic voltammograms were recorded with a 797 VA Computrace system (Metrohm, Switzerland). All measurements were performed with a conventional three-electrode configuration consisting of glassy carbon working and platinum auxiliary electrodes and a Ag/AgCl reference electrode. The solvent used in all experiments was CH_3CN or CH_2Cl_2, which was deoxygenated before use. Tetra-*n*-butylammonium hexafluorophosphate (0.05 M solution) was used as a supporting electrolyte. Redox potential values ($E_{1/2}$) were determined as (E_a + E_c)/2, where E_a and E_c are anodic and cathodic peak potentials, respectively.

[$Mo_3(CuCl)S_4Cl_3(dbbpy)_3$][$CuCl_2$], [2][$CuCl_2$]. A mixture of [**1**]Cl (0.2 g, 0.146 mmol) and CuCl (0.07 g, 0.715 mmol) in THF (20 mL) was refluxed for 5 h. The final red solution was filtered off and evaporated to dryness. The solid product was dissolved in CH_2Cl_2, and an excess of hexane was layered on the solution. Red crystals of the title compound separated. Yield: 0.19 g (79%). $C_{54}H_{72}N_6Cl_6Cu_2Mo_3S_4{\cdot}CH_2Cl_2$ (1645.81): Anal. Calcd C 40.1; H 4.5, N 5.1; found C 39.5, H 4.5, N 5.1%. ^1H NMR (500 MHz, 298 K, CD_2Cl_2): δ 9.72 and 9.62 (d, dbbpy-$H^{2,2'}$, $^3J_{HH}$ = 6.1 Hz, 3H each); 8.43 and 8.27 (d, dbbpy-$H^{5,5'}$, $^4J_{HH}$ = 1.8 Hz, 3H each); 7.73 and 7.54 (dd, dbbpy-$H^{3,3'}$, $^3J_{HH}$ = 6.1 Hz, $^4J_{HH}$ = 1.8 Hz, 3H each); 1.52 and 1.44 (s, ^{t}Bu, 27H each). $^{13}C\{^1H\}$ NMR (150 MHz, 298 K, CD_2Cl_2): δ 161.3 (s, dbbpy-$C^{4,4'}$); 156.8 (s, dbbpy-$C^{2,2'}$); 154.8 and 153.3 (s, dbbpy-$C^{6,6'}$); 125.4 and 123.8 (s, dbbpy-$C^{3,3'}$); 122.1 and 120.4 (s, dbbpy-$C^{5,5'}$); 35.6 (s, $\underline{C}(CH_3)_3$), 30.0 (s, $C(\underline{C}H_3)_3$). IR (KBr pellet): υ = 3448 (w, sh), 3089 (w), 2964 (vs), 2908 (s), 2871 (s), 1614 (vs), 1545 (m), 1483 (s), 1466 (m), 1412 (vs), 1367 (m), 1294 (m), 1254 (s), 1204 (m), 1157 (w), 1128 (m), 1082 (s), 1055 (s), 1024 (s), 931 (w), 899 (m), 837 (m), 743 (w), 605 (m), 551 (w), 492 (w), 446 (w), 424 (w) cm^{-1}. ESI-MS (+; CH_2Cl_2/CH_3CN): m/z = 1425 $[M]^+$, m/z = 1328 $[M\text{-}CuCl]^+$. CV (CH_3CN, vs Ag/AgCl): $E_{1/2}$ = −0.047 V (ΔE_p = 0.077 V), $E_{1/2}$ = 0.55 V (ΔE_p = 0.15 V) at a potential sweep rate of 0.1 V/s.

[$Mo_3(CuCl)S_4Cl_3(dbbpy)_3$][$PF_6$], [2][$PF_6$]. A mixture of [**1**]Cl (0.2 g, 0.146 mmol) and CuCl (0.07 g, 0.715 mmol) in THF (20 mL) was refluxed for 5 h. The resulting red solution was filtered and evaporated to dryness. The solid product was dissolved in CH_2Cl_2, and the solution was loaded onto a silica gel column. After it was washed with CH_2Cl_2, elution with a solution of KPF_6 in acetone (10 mg/mL) afforded a concentrated red solution. This solution was evaporated to dryness, redissolved in CH_2Cl_2, and filtered to eliminate the inorganic salts. Finally the resulting solution was allowed to evaporate slowly in air to give 0.13 g (56%) of dark red solid. ^1H NMR (500 MHz, 298 K, CD_2Cl_2): δ 9.72 and 9.62 (d, dbbpy-$H^{2,2'}$, $^3J_{HH}$ = 6.1 Hz, 3H each); 8.43 and 8.25 (d, dbbpy-$H^{5,5'}$, $^4J_{HH}$ = 1.8 Hz, 3H each); 7.73 and 7.54 (dd, dbbpy-$H^{3,3'}$, $^3J_{HH}$ = 6.1 Hz, $^4J_{HH}$ = 1.8 Hz, 3H each); 1.51 and 1.43 (s, ^{t}Bu, 27H each). ^{19}F NMR (470 MHz, 298 K, CD_2Cl_2) δ −73.13 (d, $^1J_{FP}$ = 713 Hz, P$\underline{F}_6$). ^{31}P NMR (161.9 MHz, 298 K, CD_2Cl_2) δ −145.4 (sept, $^1J_{FP}$ = 713 Hz, $\underline{P}F_6$). IR (KBr pellet): υ = 3227 (w), 3133 (w), 3094 (w), 3067 (w), 2965 (vs), 2911 (s), 2874 (s), 2019 (w), 1919 (w), 1616 (vs), 1545 (m), 1483 (s), 1464 (s), 1412 (vs), 1367 (s), 1312 (m), 1294 (m), 1256 (s), 1204 (m), 1157 (w), 1128 (w), 1078 (w), 1026 (s), 903 (s), 837 (vs, PF_6), 740 (m), 604 (s), 557 (vs, PF_6), 488 (w). CV (CH_2Cl_2, vs Ag/AgCl): $E_{1/2}$ = −0.071 V (ΔE_p = 0.107 V) at a potential sweep rate of 0.1 V/s.

Structural Determination. Single crystals of [**2**][$CuCl_2$]·$4CH_2Cl_2$ suitable for X-ray analysis were obtained by recrystallization of [**2**][$CuCl_2$] from CH_2Cl_2/hexane mixture. The diffraction data were collected on a Bruker Apex Duo diffractometer with Mo Kα radiation (λ = 0.710 73 Å), by doing φ and ω scans of narrow (0.5°) frames at 150 K. The structure was solved by direct methods and refined by full-matrix least-squares treatment against $|F|^2$ in anisotropic approximation with SHELXTL programs set.[57] Absorption corrections were applied empirically with SADABS program.[58] In the structure all *tert*-Bu groups of dbbpy ligands are disordered over several positions as a result of combination of different orientations of this group inside the crystal. This did not allow to refine carbon atoms of *tert*-Bu groups in the anisotropic approximation. The hydrogen atoms were refined in their geometrically calculated positions; a riding model was used for this purpose. The crystal structure has very large accessible voids, which are occupied with highly disordered molecules of CH_2Cl_2. To observe a current composition of the crystal a SQUEESE procedure[59] and a PLATON program set[60] were used. It gives 660 e per the unit cell that can be assigned as four molecules of CH_2Cl_2 per formula unit. Crystallographic data and refinement details are given in Table S3. Additional crystallographic information is available in the Supporting Information.

Kinetics Experiments. The kinetics experiments were performed with an Applied Photophysics SX-17MV stopped-flow spectrometer provided with a PDA1 photodiode array detector. All experiments were performed at 25.0 ± 0.1 °C by mixing a solution of [**2**][$CuCl_2$] with different halide ligands (Pr_4NCl, Bu_4PBr, Bu_4NF) using CH_2Cl_2 as solvent under a nitrogen atmosphere. The halide concentration range was (0.19−1.10) × 10^{-3} M in the stopped-flow enough to ensure pseudo-first-order conditions in all experiments. The complex solutions were prepared at concentrations of ca. 3.5 × 10^{-5} M in CH_2Cl_2. Measurements were performed in the presence of ionic strength 0.05 M, adding in each case the necessary amount of Bu_4NClO_4 to the solution. In previous experiments, we checked that this salt behaved as inert. For the cryo-stopped flow experiments on the formation of [**2**], acetone solutions of [**1**](PF_6) and [Cu(CH_3CN)$_4$](BF_4) were mixed in a Biologic SF4 instrument provided with a diode array detector. In all cases the spectral changes were measured over a wide wavelength range (ca. 300−800 nm) and analyzed with the program Specfit.[61]

Computational Density Functional Theory Calculations. All DFT calculations were performed by using Gaussian 09.[62] Geometry optimizations were performed at the BP86/BS1 level of theory[63,64] without any symmetry constraint, and included the effects of the solvent (CH_3CN, ε = 35.688) self-consistently through the polarizable continuum model (PCM).[65,66] In all cases dbbpy ligands were modeled as bpy, that is, substituting the *tert*-butyl groups in dbbpy by H atoms. Basis set system BS1 employs the SDD relativistic ECP and associated basis set for Mo, W, Cu, P, and S atoms,[67] with added polarization functions for P (ζ = 0.387) and S (ζ = 0.503),[68] and the 6-31G(d,p) basis set for Cl, Br, N, C, and H atoms.[69,70] Frequency calculations were performed at this level of theory for all stationary points both to characterize them as either minima or transition states, and to obtain the corrections required to generate free energy values (at 298.15 K and 1 atm). To obtain improved energetic values all energies were recomputed through single-point calculations with a larger basis set system BS2 and also including solvent effects (PCM method). BS2 only differs from BS1 in the employment of the 6-311+G(2d,2p) basis set for Cl, Br, N, C, and H atoms. Solution free energies are thus based on BS2(PCM) energies and include electronic to free energy corrections as well as dispersion corrections, the latter calculated using Grimme's D3(BJ) parameter set.[71,72]

Potential energy surfaces for the selected substitution processes (see Supporting Information) were calculated at the BP86/BS1(PCM) level of theory by constructing a grid with varying Mo−Cl and Mo−X

DOI: 10.1021/acs.inorgchem.6b01878
Inorg. Chem. 2016, 55, 9912−9922

(X = Br, F) distances and fully optimizing all remaining variables. Molecular orbital compositions were determined using the QMForge program.[73] Computed structures are illustrated using CYLview.[74]

■ ASSOCIATED CONTENT

Supporting Information

The Supporting Information is available free of charge on the ACS Publications website at DOI: 10.1021/acs.inorgchem.6b01878. Further details may be obtained from the Cambridge Crystallographic Data Center on quoting the depository number CCDC 1476284. Copies of this information may be obtained free of charge from http://www.ccdc.cam.ac.uk.

Additional NMR, ESI-MS, and kinetics results. Cyclic voltammogram of $[Mo_3S_4Cl_3(dbbpy)_3]Cl$. Composition of the HOMO and LUMO orbitals of $[Mo_3S_4Cl_3(bpy)_3]^+$ and $[Mo_3S_4Cl_3(bpy)_3]$, as well as Cartesian coordinates of DFT-optimized structures and associated thermodynamic data. (PDF)

X-ray crystallographic data (excluding structure factors) for $[\mathbf{2}][CuCl_2]\ 4CH_2Cl_2$. (CIF)

■ AUTHOR INFORMATION

Corresponding Authors

*E-mail: manuel.basallote@uca.es. (M.G.B.)
*E-mail: rosa.llusar@uji.es. (R.L.)
*E-mail: gushchin@niic.nc.ru. (A.L.G.)
*E-mail: emilio.bustelo@uca.es. (E.B.)

Author Contributions

⊥J.A.P.-C., Y.A.L., and E.G. contributed equally to this work.

Notes

The authors declare no competing financial interest.

■ ACKNOWLEDGMENTS

The financial support of the Spanish Ministerio de Economía y Competividad and FEDER funds (Project Nos. CTQ2015-65707-C2-2-P and CTQ2015-65207-P) and the Russian Foundation for Basic Research (Grant No. 15-03-02775a) is gratefully acknowledged. The authors also are grateful to the SCCYT of the Univ. de Cádiz and the SCIC of the Univ. Jaume I for providing the NMR and mass spectrometry facilities, respectively.

■ REFERENCES

(1) Seino, H.; Hidai, M. Catalytic functions of cubane-type M_4S_4 clusters. *Chem. Sci.* **2011**, *2* (5), 847−857.

(2) Hernandez-Molina, R.; Sokolov, M. N.; Sykes, A. G. Behavioral Patterns of Heterometallic Cuboidal Derivatives of $[M_3Q_4(H_2O)_9]^{4+}$ (M = Mo, W; Q = S, Se). *Acc. Chem. Res.* **2001**, *34* (3), 223−230.

(3) Hidai, M.; Kuwata, S.; Mizobe, Y. Synthesis and Reactivities of Cubane-Type Sulfido Clusters Containing Noble Metals. *Acc. Chem. Res.* **2000**, *33* (1), 46−52.

(4) Shibahara, T. Synthesis of sulfur bridged molybdenum and tungsten coordination compounds. *Coord. Chem. Rev.* **1993**, *123*, 73−147.

(5) Akashi, H.; Shibahara, T. Molybdenum−copper−sulfur Mo_3CuS_4 cubes. *Inorg. Chim. Acta* **2000**, *300*−*302*, 572−580.

(6) Shibahara, T.; Akashi, H.; Kuroya, H. Preparation and x-ray structure of a mixed-metal double cubane-type aqua ion, $[(H_2O)_9Mo_3S_4CuCuS_4Mo_3(H_2O)_9]^{8+}$. *J. Am. Chem. Soc.* **1988**, *110* (10), 3313−3314.

(7) Nasreldin, M.; Li, Y.-J.; Mabbs, F. E.; Sykes, A. G. Preparation and Properties of the Heterometallic Cuboidal Cluster $[Mo_3CuS_4(H_2O)_{10}]^{5+}$ and Comparisons with $[Mo_3CuS_4(H_2O)_{10}]^{4+}$. *Inorg. Chem.* **1994**, *33* (19), 4283−4289.

(8) Guillamón, E.; Llusar, R.; Pérez-Prieto, J.; Stiriba, S.-E. Insight into the mechanism of diazocompounds transformation catalyzed by hetero cuboidal clusters $[Mo_3CuQ_4(MeBPE)_3X_4]^+$, (Q = S, Se; X = Cl, Br): The catalytically active species. *J. Organomet. Chem.* **2008**, *693* (8−9), 1723−1727.

(9) Feliz, M.; Guillamón, E.; Llusar, R.; Vicent, C.; Stiriba, S.-E.; Pérez-Prieto, J.; Barberis, M. Unprecedented Stereoselective Synthesis of Catalytically Active Chiral Mo_3CuS_4 Clusters. *Chem. - Eur. J.* **2006**, *12* (5), 1486−1492.

(10) Yifan, Z.; Huqiang, Z.; Xintao, W.; Jiaxi, L. The synthesis and crystal structure of a cubane-like tungsten copper sulphur cluster, $[W_4CuS_4\{_2P(OEt)_2\}_3(I)(\mu_2\text{-}PhCO_2)\ (MeCN)]$. *Transition Met. Chem.* **1989**, *14* (3), 161−164.

(11) Diller, H.; Keck, H.; Kuchen, W.; Mootz, D.; Wiskemann, R. *Z. Naturforsch., B: J. Chem. Sci.* **1993**, *48* (3), 291−296.

(12) Herbst, K.; Monari, M.; Brorson, M. Facile formation of a heterobimetallic cluster with a cubane-like $[Mo_3S_4Cu]^{5+}$ core. *Inorg. Chim. Acta* **2004**, *357* (3), 895−899.

(13) Lu, S.-F.; Chen, H.-B.; Huang, J.-Q.; Wu, Q.-J.; Sun, Q.-L.; Li, J.; Lu, J.-X. Ligand-cluster reactivity and structure relationship; the synthesis, structural characterization and properties of two new Mo-Cu-S cluster compounds. *Inorg. Chim. Acta* **1995**, *232* (1−2), 43−50.

(14) Gushchin, A. L.; Sokolov, M. N.; Kovalenko, K. A.; Peresypkina, E. V.; Virovets, A. V.; Alferova, N. I.; Fedin, V. P. Cubane pyridine-acetylacetonate cluster complexes with the $M_3CuS_4^{5+}$ core (M = Mo, W). *Russ. J. Coord. Chem.* **2009**, *35* (6), 395−400.

(15) Zhao, X.; Zhou, F.; Liu, Q.; Chen, Q.-F.; Yang, J.-Y.; Zhang, W.-H.; Song, Y.-L.; Lang, J.-P. Diverse Tp*-Capped W−Cu−S Clusters from One-Pot Assembly Involving in Situ Thiolation of Phosphines. *Inorg. Chem.* **2016**, *55* (4), 1861−1871.

(16) Zhang, W.-H.; Liu, Q.; Lang, J.-P. Heterometallic transition metal clusters and cluster-supported coordination polymers derived from Tp- and Tp*-based Mo(W) sulfido precursors. *Coord. Chem. Rev.* **2015**, *293*−*294*, 187−210.

(17) Liu, Q.; Ren, Z.-G.; Deng, L.; Zhang, W.-H.; Zhao, X.; Sun, Z.-R.; Lang, J.-P. Solvent effect-driven assembly of W/Cu/S cluster-based coordination polymers from the cluster precursor $[Et_4N][Tp^*WS_3(CuBr)_3]$ and CuCN: isolation, structures and enhanced NLO responses. *Dalton Trans.* **2015**, *44* (1), 130−137.

(18) Zhou, L.-K.; Liu, Q.; Zhao, X.; Hu, F.-L.; Liu, S.-C.; Ren, Z.-G.; Sun, Z.-R.; Lang, J.-P. Six $[Tp^*WS_3Cu_2]$-based clusters derived from $[Et_4N][Tp^*WS_3]$, Cu(I) salts and phosphine ligands: syntheses, structures and enhanced third-order NLO properties. *Dalton Trans.* **2014**, *43* (12), 4734−4744.

(19) Wei, Z.-H.; Ni, C.-Y.; Li, H.-X.; Ren, Z.-G.; Sun, Z.-R.; Lang, J.-P. $[PyH][\{TpMo(\mu_3\text{-}S)_4Cu_3\}_4(\mu_{12}\text{-}I)]$: a unique tetracubane cluster derived from the S-S bond cleavage and the iodide template effects and its enhanced NLO performances. *Chem. Commun.* **2013**, *49* (42), 4836−4838.

(20) Algarra, A. G.; Feliz, M.; Fernández-Trujillo, M. J.; Llusar, R.; Safont, V. S.; Vicent, C.; Basallote, M. G. Unprecedented Solvent-Assisted Reactivity of Hydrido W_3CuS_4 Cubane Clusters: The Non-Innocent Behaviour of the Cluster-Core Unit. *Chem. - Eur. J.* **2009**, *15* (18), 4582−4594.

(21) Pedrajas, E.; Sorribes, I.; Junge, K.; Beller, M.; Llusar, R. A Mild and Chemoselective Reduction of Nitro and Azo Compounds Catalyzed by a Well-Defined Mo_3S_4 Cluster Bearing Diamine Ligands. *ChemCatChem* **2015**, *7* (17), 2675−2681.

(22) Gushchin, A. L.; Laricheva, Y. A.; Abramov, P. A.; Virovets, A. V.; Vicent, C.; Sokolov, M. N.; Llusar, R. Homoleptic Molybdenum Cluster Sulfides Functionalized with Noninnocent Diimine Ligands: Synthesis, Structure, and Redox Behavior. *Eur. J. Inorg. Chem.* **2014**, *2014* (25), 4093−4100.

(23) Gushchin, A. L.; Laricheva, Y. A.; Piryazev, D. A.; Sokolov, M. N. Mixed-ligand cluster $[Mo_3S_4(Dtp)_2(\mu\text{-}AcO)Cl(Me_2Bipy)]$: Synthesis and structure. *Russ. J. Coord. Chem.* **2014**, *40* (1), 5−9.

DOI: 10.1021/acs.inorgchem.6b01878
Inorg. Chem. 2016, 55, 9912−9922

(24) Pino-Chamorro, J. Á.; Laricheva, Y. A.; Guillamon, E.; Fernández-Trujillo, M. J.; Bustelo, E.; Gushchin, A. L.; Shmelev, N. Y.; Abramov, P. A.; Sokolov, M. N.; Llusar, R.; Basallote, M. G.; Algarra, A. G. Cycloaddition of Alkynes to Diimino Mo_3S_4 Cubane-Type Clusters: A combined experimental and theoretical approach. *New J. Chem.* **2016**, *40*, 7872−7880.
(25) Nasreldin, M.; Routledge, C. A.; Sykes, A. G. Preparation and aqueous solution properties of the heterometallic cuboidal complex $[W_3CuS_4(H_2O)_{10}]^{5+}$. *J. Chem. Soc., Dalton Trans.* **1994**, *19*, 2809−2814.
(26) Jaramillo, T. F.; Bonde, J.; Zhang, J.; Ooi, B.-L.; Andersson, K.; Ulstrup, J.; Chorkendorff, I. Hydrogen Evolution on Supported Incomplete Cubane-type $[Mo_3S_4]^{4+}$ Electrocatalysts. *J. Phys. Chem. C* **2008**, *112* (45), 17492−17498.
(27) Kristensen, J.; Zhang, J.; Chorkendorff, I.; Ulstrup, J.; Ooi, B. L. Assembled monolayers of $Mo_3S_4^{4+}$ clusters on well-defined surfaces. *Dalton Trans.* **2006**, *33*, 3985−3990.
(28) Algarra, A. G.; Basallote, M. G.; Fernández-Trujillo, M. J.; Llusar, R.; Safont, V. S.; Vicent, C. The Structure of ($[W_3Q_4X_3(dmpe)_3]^+$, Y^-) Ion Pairs (Q = S, Se; X = H, OH, Br; Y = BF_4, PF_6, dmpe = $Me_2PCH_2CH_2PMe_2$) in Dichloromethane Solution and the Effect of Ion-Pairing on the Kinetics of Proton Transfer to the Hydride Cluster $[W_3S_4H_3(dmpe)_3]^+$. *Inorg. Chem.* **2006**, *45* (15), 5774−5784.
(29) Algarra, A. G.; Fernández-Trujillo, M. J.; Lledós, A.; Basallote, M. G. Dihydrogen complexes: striking effect of ion pairing to BF_4^- on the rotation of coordinated dihydrogen and the ^{19}F relaxation time. *Chem. Commun.* **2009**, *30*, 4563−4565.
(30) Basallote, M. G.; Besora, M.; Castillo, C. E.; Fernández-Trujillo, M. J.; Lledós, A.; Maseras, F.; Máñez, M. A. Crucial Role of Anions on the Deprotonation of the Cationic Dihydrogen Complex trans-$[FeH(\eta^2\text{-}H_2)(dppe)_2]^+$. *J. Am. Chem. Soc.* **2007**, *129*, 6608−6618.
(31) Basallote, M. G.; Besora, M.; Durán, J.; Fernández-Trujillo, M. J.; Lledós, A.; Máñez, M. A.; Maseras, F. The Effect of the "Inert" Counteranions in the Deprotonation of the Dihydrogen Complex *trans*-$[FeH(\eta^2\text{-}H_2)(dppe)_2]^+$: Kinetic and Theoretical Studies. *J. Am. Chem. Soc.* **2004**, *126* (8), 2320−2321.
(32) Crabtree, R. H. Deactivation in Homogeneous Transition Metal Catalysis: Causes, Avoidance, and Cure. *Chem. Rev.* **2015**, *115* (1), 127−150.
(33) Lu, Z.; Han, J.; Hammond, G. B.; Xu, B. Revisiting the Influence of Silver in Cationic Gold Catalysis: A Practical Guide. *Org. Lett.* **2015**, *17* (18), 4534−4537.
(34) Wang, D.; Cai, R.; Sharma, S.; Jirak, J.; Thummanapelli, S. K.; Akhmedov, N. G.; Zhang, H.; Liu, X.; Petersen, J. L.; Shi, X. Silver Effect" in Gold(I) Catalysis: An Overlooked Important Factor. *J. Am. Chem. Soc.* **2012**, *134* (21), 9012−9019.
(35) Chen, P.; Chen, Y.; Zhou, Y.; Peng, Y.; Qu, J.; Hidai, M. Heterometallic cubane-type clusters $[M'Mo_3S_4]$ (M′ = Au, Ag and Cu): synthesis, structures and electrochemical properties. *Dalton Trans.* **2010**, *39* (24), 5658−5663.
(36) Feliz, M.; Garriga, J. M.; Llusar, R.; Uriel, S.; Humphrey, M. G.; Lucas, N. T.; Samoc, M.; Luther-Davies, B. Synthesis, Structure, and Optical-Limiting Properties of Heterobimetallic $[M_3CuS_4]$ Cuboidal Clusters (M = Mo or W) with Terminal Phosphine Ligands. *Inorg. Chem.* **2001**, *40* (24), 6132−6138.
(37) Gushchin, A.; Llusar, R.; Recatalá, D.; Abramov, P. First heteroleptic Mo_3S_7 clusters containing non-innocent phenanthroline ligands. *Russ. J. Coord. Chem.* **2012**, *38* (3), 173−177.
(38) Gushchin, A. L.; Sokolov, M. N.; Peresypkina, E. V.; Virovets, A. V.; Kozlova, S. G.; Zakharchuk, N. F.; Fedin, V. P. Crystal Structure, Electronic Structure, and Solid-State Electrochemistry of Cluster Complexes of $M_3Se_7^{4+}$ (M = Mo, W) with Noninnocent o-Phenanthroline and Se_2^{2-} Ligands. *Eur. J. Inorg. Chem.* **2008**, *2008*, 3964−3969.
(39) Jagner, S.; Helgesson, G. On the Coordination Number of the Metal in Crystalline Halogenocuprates(I) and Halogenoargentates(I). In *Advances in Inorganic Chemistry;* Sykes, A.G., Ed.; Academic Press, 1991; Vol. *37*, pp 1−45 and references therein.
(40) Wang, J.-G.; Kang, H.-X.; Zheng, X.-Y. *Z. Kristallogr.−New Cryst. Struct.* **2005**, *220*, 597−598.
(41) Feliz, M.; Guillamón, E.; Llusar, R.; Vicent, C.; Stiriba, S.-E.; Pérez-Prieto, J.; Barberis, M. Unprecedented Stereoselective Synthesis of Catalytically Active Chiral Mo_3CuS_4 Clusters. *Chem. - Eur. J.* **2006**, *12* (5), 1486−1492.
(42) Wu, X.; Lu, S.; Zu, L.; Wu, Q.; Lu, J. The synthesis and crystal structure of a novel cubane-like molybdenum copper sulfur cluster $[Mo_3CuS_4]\cdot[S_2P(OC_2H_5)_2]_3\cdot I\cdot CH_3COO\cdot HCON(CH_3)_2$. *Inorg. Chim. Acta* **1987**, *133* (1), 39−42.
(43) Several chlorocuprate species, namely, $[CuCl_2]^-$, $[Cu_2Cl_2]^-$, and $[CuCl_3]^-$ are also seen in the negative scan of compound [**2**] $[CuCl_2]$ (see Supporting Information, Figure S6).
(44) Llusar, R.; Uriel, S. Heterodimetallic chalcogen-bridged cubane-type clusters of molybdenum and tungsten containing first-row transition metals. *Eur. J. Inorg. Chem.* **2003**, *2003* (7), 1271−1290.
(45) DFT calculations were performed using bpy ligands as models for dbbpy. See Computational Details.
(46) Burg, A.; Meyerstein, D. *Advances in Inorganic Chemistry, Vol 64: Inorganic Bioinorganic Reaction Mechanisms;* Van Eldik, R., Ed.; Elsevier Academic Press, Inc, San Diego, CA, 2012; Vol. *64*, pp 219−261.
(47) Algarra, A. G.; Fernández-Trujillo, M. J.; Basallote, M. G. A DFT and TD-DFT Approach to the Understanding of Statistical Kinetics in Substitution Reactions of M_3Q_4 (M = Mo, W; Q = S, Se) Cuboidal Clusters. *Chem. - Eur. J.* **2012**, *18* (16), 5036−5046.
(48) Beltrán, T. F.; Llusar, R.; Sokolov, M.; Basallote, M. G.; Fernández-Trujillo, M. J.; Pino-Chamorro, J. Á. Influence of the Ligand Alkyl Chain Length on the Solubility, Aqueous Speciation, and Kinetics of Substitution Reactions of Water-Soluble M_3S_4 (M = Mo, W) Clusters Bearing Hydroxyalkyl Diphosphines. *Inorg. Chem.* **2013**, *52* (15), 8713−8722.
(49) Beltrán, T. F.; Pino-Chamorro, J. Á.; Fernández-Trujillo, M. J.; Safont, V. S.; Basallote, M. G.; Llusar, R. Synthesis and Structure of Trinuclear W_3S_4 Clusters Bearing Aminophosphine Ligands and Their Reactivity toward Halides and Pseudohalides. *Inorg. Chem.* **2015**, *54* (2), 607−618.
(50) Alfonso, C.; Beltrán, T. F.; Feliz, M.; Llusar, R. Influence of the Diphosphine Coordinated to Molybdenum and Tungsten Triangular M_3S_4 Cluster Hydrides in the Catalytic Hydrodefluorination of Pentafluoropyridine. *J. Cluster Sci.* **2015**, *26* (1), 199−209.
(51) Mironov, Y. V.; Yarovoi, S. S.; Solodovnikov, S. F.; Fedorov, V. E. Coordinated bifluoride ions in the first thiofluoride molybdenum triangular cluster complex: synthesis and crystal structure of $K_5[Mo_3S_4F_7(FHF)_2]\cdot 2H_2O$. *J. Mol. Struct.* **2003**, *656* (1−3), 195−199.
(52) Kurtz, K. S.; Stevenson, K. L. Spectra and photochemistry of the chloro complexes of copper(I). *Proc. Indiana Acad. Sci.* **1985**, *90*, 187−191.
(53) Powell, K. J. *IUPAC Stability Constants Database;* Academic Software: Canterbury, 2000.
(54) Tsuboyama, A.; Kuge, K.; Furugori, M.; Okada, S.; Hoshino, M.; Ueno, K. Photophysical Properties of Highly Luminescent Copper(I) Halide Complexes Chelated with 1,2-Bis(diphenylphosphino)benzene. *Inorg. Chem.* **2007**, *46* (6), 1992−2001.
(55) Hashimoto, M.; Igawa, S.; Yashima, M.; Kawata, I.; Hoshino, M.; Osawa, M. Highly Efficient Green Organic Light-Emitting Diodes Containing Luminescent Three-Coordinate Copper(I) Complexes. *J. Am. Chem. Soc.* **2011**, *133* (27), 10348−10351.
(56) Kang, L.; Chen, J.; Teng, T.; Chen, X.-L.; Yu, R.; Lu, C.-Z. Experimental and theoretical studies of highly emissive dinuclear Cu(I) halide complexes with delayed fluorescence. *Dalton Trans.* **2015**, *44* (25), 11649−11659.
(57) Sheldrick, G. M. A short story of SHELX. *Acta Crystallogr., Sect. A: Found. Crystallogr.* **2008**, *64*, 112−122.
(58) Sheldrick, G. M. *SADABS*; University of Göttingen: Germany, 1996.
(59) van der Sluis, P.; Spek, A. L. BYPASS: an effective method for the refinement of crystal structures containing disordered solvent regions. *Acta Crystallogr., Sect. A: Found. Crystallogr.* **1990**, *46* (3), 194−201.

DOI: 10.1021/acs.inorgchem.6b01878
Inorg. Chem. 2016, 55, 9912−9922

(60) Spek, A. Structure validation in chemical crystallography. *Acta Crystallogr., Sect. D: Biol. Crystallogr.* **2009**, *65* (2), 148−155.
(61) Binstead, R. A.; Jung, B.; Zuberbühler, A. D. *SPECFIT-32*; Spectrum Software Associates: Chappel Hill, 2000.
(62) Frisch, M. J., Trucks, G. W.; Schlegel, H. B.; Scuseria, G. E.; Robb, M. A.; Cheeseman, J. R.; Scalmani, G.; Barone, V.; Mennucci, B.; Petersson, G. A.; Nakatsuji, H.; Caricato, M.; Li, X.; Hratchian, H. P.; Izmaylov, A. F.; Bloino, J.; Zheng, G.; Sonnenberg, J. L.; Hada, M.; Ehara, M.; Toyota, K.; Fukuda, R.; Hasegawa, J.; Ishida, M.; Nakajima, T.; Honda, Y.; Kitao, O.; Nakai, H.; Vreven, T.; Montgomery, J. A., Jr.; Peralta, J. E.; Ogliaro, F.; Bearpark, M.; Heyd, J. J.; Brothers, E.; Kudin, K. N.; Staroverov, V. N.; Kobayashi, R.; Normand, J.; Raghavachari, K.; Rendell, A.; Burant, J. C.; Iyengar, S. S.; Tomasi, J.; Cossi, M.; Rega, N.; Millam, N. J.; Klene, M.; Knox, J. E.; Cross, J. B.; Bakken, V.; Adamo, C.; Jaramillo, J.; Gomperts, R.; Stratmann, R. E.; Yazyev, O.; Austin, A. J.; Cammi, R.; Pomelli, C.; Ochterski, J. W.; Martin, R. L.; Morokuma, K.; Zakrzewski, V. G.; Voth, G. A.; Salvador, P.; Dannenberg, J. J.; Dapprich, S.; Daniels, A. D.; Farkas, Ö.; Foresman, J. B.; Ortiz, J. V.; Cioslowski, J.; Fox, D. J. *Gaussian 09,* Revision D.01; Gaussian, Inc: Wallingford, CT, 2013.
(63) Becke, A. D. Density-Functional Thermochemistry. III. The Role Of Exact Exchange. *J. Chem. Phys.* **1993**, *98* (7), 5648−5652.
(64) Lee, C. T.; Yang, W. T.; Parr, R. G. Development Of The Colle-Salvetti Correlation-Energy Formula Into A Functional Of The Electron-Density. *Phys. Rev. B: Condens. Matter Mater. Phys.* **1988**, *37* (2), 785−789.
(65) Tomasi, J.; Mennucci, B.; Cammi, R. Quantum mechanical continuum solvation models. *Chem. Rev.* **2005**, *105* (8), 2999−3093.
(66) Cossi, M.; Scalmani, G.; Rega, N.; Barone, V. New developments in the polarizable continuum model for quantum mechanical and classical calculations on molecules in solution. *J. Chem. Phys.* **2002**, *117* (1), 43−54.
(67) Andrae, D.; Haussermann, U.; Dolg, M.; Stoll, H.; Preuss, H. *Theor. Chim. Acta* **1990**, *77*, 123−141.
(68) Hollwarth, A.; Bohme, M.; Dapprich, S.; Ehlers, A. W.; Gobbi, A.; Jonas, V.; Kohler, K. F.; Stegmann, R.; Veldkamp, A.; Frenking, G. A Set Of D-Polarization Functions For Pseudo-Potential Basis-Sets Of The Main-Group Elements Al-Bi And F-Type Polarization Functions For Zn, Cd, Hg. *Chem. Phys. Lett.* **1993**, *208* (3−4), 237−240.
(69) Hehre, W. J.; Ditchfield, R.; Pople, J. A. Self-Consistent Molecular Orbital Methods. XII. Further Extensions of Gaussian—Type Basis Sets for Use in Molecular Orbital Studies of Organic Molecules. *J. Chem. Phys.* **1972**, *56* (5), 2257−2261.
(70) Hariharan, P. C.; Pople, J. A. Influence of polarization functions on molecular-orbital hydrogenation energies. *Theor. Chim. Acta* **1973**, *28* (3), 213−222.
(71) Grimme, S.; Antony, J.; Ehrlich, S.; Krieg, H. A consistent and accurate ab initio parametrization of density functional dispersion correction (DFT-D) for the 94 elements H-Pu. *J. Chem. Phys.* **2010**, *132* (15), 154104.
(72) Grimme, S.; Ehrlich, S.; Goerigk, L. Effect of the damping function in dispersion corrected density functional theory. *J. Comput. Chem.* **2011**, *32* (7), 1456−1465.
(73) Tenderholt, A. L. *QMForge, v. 2.1;* Stanford University: Stanford, CA, 2007.
(74) Legault, C. *CYLview v1.0b;* Université de Sherbrooke, 2009.

DOI: 10.1021/acs.inorgchem.6b01878
Inorg. Chem. 2016, 55, 9912−9922